



HAL
open science

Determination of Successive Complexation Constants in an Ionic Liquid: Complexation of UO_2^{2+} with NO_3^- in $\text{C}_4\text{-mimTf}_2\text{N}$ Studied by UV-Vis Spectroscopy

Sylvia Georg, Isabelle Billard, Ali Ouadi, Laetitia Petitjean, Michel Picquet, Clotilde Gaillard, Vitaly Solov'ev

► To cite this version:

Sylvia Georg, Isabelle Billard, Ali Ouadi, Laetitia Petitjean, Michel Picquet, et al.. Determination of Successive Complexation Constants in an Ionic Liquid: Complexation of UO_2^{2+} with NO_3^- in $\text{C}_4\text{-mimTf}_2\text{N}$ Studied by UV-Vis Spectroscopy. *Journal of Physical Chemistry B*, 2010, 114 (12), pp.4276-4282. 10.1021/jp9107624 . in2p3-00734038

HAL Id: in2p3-00734038

<https://hal.in2p3.fr/in2p3-00734038>

Submitted on 12 Oct 2021

HAL is a multi-disciplinary open access archive for the deposit and dissemination of scientific research documents, whether they are published or not. The documents may come from teaching and research institutions in France or abroad, or from public or private research centers.

L'archive ouverte pluridisciplinaire **HAL**, est destinée au dépôt et à la diffusion de documents scientifiques de niveau recherche, publiés ou non, émanant des établissements d'enseignement et de recherche français ou étrangers, des laboratoires publics ou privés.



Distributed under a Creative Commons Attribution - NonCommercial 4.0 International License

Determination of Successive Complexation Constants in an Ionic Liquid: Complexation of UO_2^{2+} with NO_3^- in $\text{C}_4\text{-mimTf}_2\text{N}$ Studied by UV–Vis Spectroscopy

Sylvia Georg,[†] Isabelle Billard,^{*,†} Ali Ouadi,[†] Clotilde Gaillard,[‡] Laetitia Petitjean,[§] Michel Picquet,[§] and Vitaly Solov'ev[⊥]

IPHC, UMR 7178 CNRS-IN2P3 et Université de Strasbourg, 23 rue du Loess, 67037 Strasbourg cedex 2, France, IPN Lyon, Université Lyon I, 4 rue E. Fermi, 69622 Villeurbanne Cedex, France, Institut de Chimie Moléculaire de l'Université de Bourgogne, UMR 5260 CNRS - Université de Bourgogne, 9 avenue A. Savary, BP 47870, 21078 Dijon, cedex, France, and Institute of Physical Chemistry and Electrochemistry of Russian Academy of Sciences, Leninsky pr. 31a, 119991 Moscow, Russia

The complexation of UO_2^{2+} with NO_3^- has been investigated in the ionic liquid 1-butyl-3-methylimidazolium bis(trifluoromethylsulfonyl)imide by UV–vis spectroscopy at $T = 18.5^\circ\text{C}$. The complexation is evidenced through the appearance of four peaks at 425, 438, 453, and 467 nm. EXAFS data indicate that the trinitrate complex, $\text{UO}_2(\text{NO}_3)_3^-$, is dominating the speciation for a reagent ratio of $[\text{NO}_3^-]/[\text{UO}_2^{2+}] > 3$. Assuming three successive complexation steps, the conditional stability constants are calculated, the individual absorption spectra are derived, and a speciation plot is presented.

Introduction

Ionic liquids (ILs) are a class of solvents,¹ composed of an (in)organic cation (most frequently imidazolium, pyrrolidinium, tetraalkylammonium, etc.) and an inorganic anion (PF_6^- , BF_4^- , Cl^- , CF_3SO_3^- , $(\text{CF}_3\text{SO}_2)_2\text{N}^-$, etc.), with so many industrially beneficial properties (in particular, ILs are nonflammable and nonvolatile, thus being often called “green solvents”) that an increasing number of publications is devoted to their study as replacement solvents in all fields of chemistry (electrochemistry, catalysis, synthesis, liquid/liquid extraction, etc.).^{2–6} Some very fundamental or basic chemical aspects are also covered, such as solvation, complexation, or extraction mechanism of various ions or molecules in ILs.^{3,7} Besides the potential of ILs for innovative chemistry, owing to the “onion shell” structure^{8–10} of the ionic solvation sphere in these media, ILs represent a real challenge for theoreticians because of their intrinsic (chemical) complexity. At the same time, ILs offer a unique chemical media to test the various correction laws (either empirical or analytical) for activity coefficients at very high ionic strengths that have been proposed and studied for the aqueous case.^{11–13} Surprisingly enough, however, to our knowledge, not a single paper is concerned with the determination of equilibrium chemical constants in ILs, which is a prerequisite to the study of ionic strength effects and Coulombic interactions in ILs.

Our group is interested in actinide and lanthanide chemistry in ILs, both on fundamental and applied aspects.^{14–18} In this respect, we intended to experimentally derive the equilibrium constants of an actinide cation with a charged ligand in a “classical” IL, 1-butyl-3-methylimidazolium bis(trifluoromethylsulfonyl)imide (further denoted as $\text{C}_4\text{-mimTf}_2\text{N}$, Tf_2N^- standing for the $(\text{CF}_3\text{SO}_2)_2\text{N}^-$ anion and $\text{C}_4\text{-mim}^+$ being the

imidazolium based cation). The uranyl cation, UO_2^{2+} , has been chosen as the reacting moiety, based on its well-defined UV–vis spectra and the amount of literature data on complexation in various solvents by UV–vis spectroscopy, that can be used for comparison purposes.^{19–22} The choice of the ligand relied on various considerations. Usually (i.e., in water, acetonitrile, or acetone), successive complexation occurs, eventually up to a limiting complex such as $\text{UO}_2\text{Cl}_4^{2-}$. In the case of chloride, four successive complexation reactions have to be considered, rendering the data analysis rather complex. We have already shown that UO_2SO_4 and $(\text{UO}_2)_3(\text{PO}_4)_2$ are not soluble in $\text{C}_4\text{-mimTf}_2\text{N}$,^{23,24} so that we finally selected the nitrate anion NO_3^- as the ligand, leading to a limiting complex of 1:3 stoichiometry only, which is of interest to studies related to the nuclear fuel cycle and has already been partially studied in $\text{C}_4\text{-mimTf}_2\text{N}$.^{24–26}

In this paper, we present UV–vis data on the successive complexation of the uranyl cation UO_2^{2+} with nitrate anions NO_3^- in the ionic liquid $\text{C}_4\text{-mimTf}_2\text{N}$ as the solvent. Both reacting moieties have been introduced as salts, the counterion being either $\text{C}_4\text{-mim}^+$ or Tf_2N^- (i.e., $\text{UO}_2(\text{Tf}_2\text{N})_2$ and $\text{C}_4\text{-mimNO}_3$ were used as reagents) in order to suppress the possible effect of “spectator ions” that cannot be avoided in usual neutral solvents. Complexation constants have been derived from UV–vis spectrophotometric data in the spectral range of 350–490 nm using either a dedicated approach or the CHEMQUI program as a general method for computations of equilibrium constants from experimental results of physico-chemical measurements.

Experimental Section

Uranyl Salt $\text{UO}_2(\text{Tf}_2\text{N})_2$. The synthesis procedure is partially based on the work of Nockemann and co-workers.²⁶ HTf_2N (95% Aldrich, white solid, highly hygroscopic) is used as received. It is dissolved in ultrapure water (5 mL for 5 g) to give an acidic solution. UO_3 (~350 mg) is dissolved in 2.5 mL of this acidic solution, which is thereafter mechanically shaken for 18 h until total dissolution of the solid. The resulting pale-

* To whom correspondence should be addressed. E-mail: isabelle.billard@ires.in2p3.fr. Phone: +33388106401. Fax: +33388106431.

[†] UMR 7178 CNRS-IN2P3 et Université de Strasbourg.

[‡] Université Lyon I.

[§] UMR 5260 CNRS - Université de Bourgogne.

[⊥] Institute of Physical Chemistry and Electrochemistry of Russian Academy of Sciences.

yellow solution is then dried under vacuum in a two-step procedure; first, the pressure is at $p = 3.5 \times 10^{-2}$ mbar until solidification starts, and then, it is at $p = 5 \times 10^{-7}$ mbar for ~ 60 h. All of the drying process is achieved without heating, but the glass container is embedded in a beaker of water at room temperature to avoid ice formation on the outside. No further purification is performed as the boiling point of HTf_2N is $T_b = 91$ °C, allowing evaporation of the acid in excess. The solid formed is pale-yellow and highly hygroscopic. Once the salt is prepared, it is kept in a closed glass tube under vacuum and is dried thoroughly prior to any use to ensure reproducibility of the UV-vis data.

C₄-mimNO₃. C₄-mimNO₃ is obtained by adaptation of the halogenide-free procedures described by Tkatchenko and co-workers²⁷ and Rogers and co-workers.²⁸ HNO₃ (68% solution in water, Acros Organics) is used as received. Acetonitrile (99.9%, Carlo Erba, HPLC grade) is distilled under argon over CaH₂ prior to use. Analyses are performed at the PACSMUB (Université de Bourgogne, France) on Bruker Avance 300 and 500 MHz NMR spectrometers, on a Bruker Vector 22 FT-IR spectrometer equipped with a Golden-Gate ATR accessory, and on a Fisons Instruments EA1108 for elemental analysis. 1-Butyl-3-methylimidazolium-2-carboxylate²⁷ (10.71 g, 58.8 mmol) is dissolved in 100 mL of distilled water in a two-necked round-bottom flask equipped with a reflux condenser under argon. To this solution, a diluted solution of HNO₃ (3.89 mL, 68%, 58.8 mmol, 1 equiv) in 100 mL of distilled water is added through a dropping funnel over a 5 min period at room temperature. The mixture is stirred 3 h at 100 °C and then allowed to cool to room temperature, and water is evaporated under vacuum ($p = 2 \times 10^{-2}$ mbar) at 35 °C. The resulting pale-yellow C₄-mimNO₃ is further dried under vacuum at 60 °C overnight, slowly turning into a deep-yellow-to-brown oil. Decolorization is subsequently performed by solubilizing C₄-mimNO₃ in 15 mL of acetonitrile and stirring this solution for 1 h over a small amount of activated charcoal. Filtration over a plug of Celite and evaporation of the solvent at room temperature under vacuum affords 11.292 g (95% yield) of C₄-mimNO₃ as a pale-yellow oil, slowly crystallizing at room temperature. A repeated drying/degassing procedure (see next section for description) leads to a yellow oil that does not crystallize any more. ¹H NMR (500.13 MHz, D₂O): $\delta = 8.68$ (br s, 1 H, NCHN), 7.46 (t, 1 H, $J = 2$ Hz, N-CH=CH-N), 7.41 (t, 1 H, $J = 2$ Hz, N-CH=CH-N), 4.18 (t, 2 H, $J = 7$ Hz, N-CH₂), 3.87 (s, 3 H, N-CH₃), 1.83 (m, 2 H, N-CH₂-CH₂), 1.29 (m, 2 H, CH₂-CH₃), 0.90 (t, 3 H, $J = 7.5$ Hz, CH₂-CH₃) ppm. ¹³C{¹H} NMR (75.47 MHz, CDCl₃): $\delta = 136.8$ (NCHN), 123.4 (N-CH=CH-N), 122.3 (N-CH=CH-N), 49.1 (N-CH₂), 35.6 (N-CH₃), 31.6 (N-CH₂-CH₂), 18.9 (CH₂-CH₃), 12.9 (CH₂-CH₃) ppm. IR (ATR, neat): 3146 (w), 3095, 2960, 2875 (w), 1572, 1326 (vs), 1167 cm⁻¹. Elemental analysis (calculated for C₈H₁₅N₃O₃): C 47.34 (47.75), H 7.74 (7.51), N 20.87 (20.88) %.

Sample Preparation. The reagent concentrations of the metal ion UO₂²⁺ and the ligand NO₃⁻ were varied from 0.0096 to 0.0101 M (UO₂²⁺) and from 0 to 0.0341 M (NO₃⁻) so that the molar ratio $R = [\text{NO}_3^-]/[\text{UO}_2^{2+}]$ varied from 0 to 3.4.

C₄-mimTf₂N was purchased from Solvionic, with no further purification, and contained ~ 300 ppm of water. Two stock solutions of C₄-mimNO₃ (1 and 0.2 M) and one stock solution of UO₂(Tf₂N)₂ (10⁻² M) in C₄-mimTf₂N were prepared. This latter solution was kept on the shelves in the dark for 4 days, so that the remaining water, either from the C₄-mimTf₂N or from the uranyl salt, could equilibrate in the bulk. Then, 3 mL

aliquots of the uranyl stock solution were mixed with required quantities of one of the nitrate stock solutions to obtain the desired R ratio. The NO₃⁻ concentrations of the stock solutions were high enough to ensure a rather limited dilution of the uranyl concentration in the final solution, whatever the R value. The solution was then carefully degassed/dried for 2 h by gentle heating ($T = 60$ °C) under vacuum ($p = 3.5 \times 10^{-2}$ mbar). The heating was then stopped, and natural cooling of the solution back to ambient temperature was allowed for one additional hour, still under vacuum. The solution was then rapidly transferred to the quartz cell and measured readily after. IR measurements have confirmed that the water amount in the degassed solution is very low, that is, below the Karl Fischer detection limit of 50 ppm (less than 0.5 water molecules per uranyl units), as was already shown.²⁹

Various trials and repeated experiments have shown that this sample preparation procedure leads to the best reproducibility of the UV-vis spectra. We suggest that letting the water in the C₄-mimTf₂N solution equilibrate between the uranyl moieties and the bulk ensures an efficient degassing of the solution afterward and therefore a very low amount of remaining water that is known to eventually enter the uranyl coordination sphere.

Measurements. UV-vis spectra were recorded on a Cary 100 system (Varian). The temperature was controlled at 18.5 °C. The data were acquired in the range of 200–800 nm. The reference sample was pure dry C₄-mimTf₂N.

All uranyl solutions were followed by UV-vis spectroscopy for a few days after being prepared. While the samples were stored in the dark between two UV-vis measurements, no caution was taken to keep them away from light all of the time, especially during the drying procedure that was performed without any light protection. Although a slight change in the absorbance was observed for the lowest $R = [\text{NO}_3^-]/[\text{U(VI)}]$ values in the range of 200–400 nm during the first 24 h after sample preparation, the spectra appeared to be very stable with time (as checked up to 8 days) above 400 nm. In agreement with a previous work,²⁹ this demonstrates that the quartz cuvette and the Teflon tap are waterproof. All data presented in this work correspond to UV-vis spectra recorded 4 days or more after sample preparation.

Data Fitting. First, an attempt was made to analyze the data through the method of principal components^{30,31} in the range of 385–485 nm to determine the exact number of chemical species, but the results were not conclusive. Second, the data were fitted according to two different procedures, hereafter referred to as “monowavelength” fitting and “multiwavelength” computations, by use of the CHEMEQUI program in the latter case.

In the monowavelength case, a Fortran routine based on least-squares adjustment (CERN library) has been written to fit the variation of the absorbance as a function of R at a fixed wavelength (see Figures 1 and 2) for the two chemical models proposed (see the Modeling and Fitting Results section). The absorbance variation is obtained from the Beer’s law, and the analytical expression for the concentration of the species is obtained, with the help of the Maple software, by solving the system of mass action laws and mass-balance equations. The unknown parameters are the various equilibrium constants β_i and the individual molar absorption ϵ_i at the chosen wavelength.

In the multiwavelength computations, the computer program CHEMEQUI, which is appropriated for the treatment of experimental data obtained via different physicochemical methods,³² was used to calculate the stability constants and the molar absorbance values from the spectrophotometric data. In the calculations, the vector β of the unknown stability constants

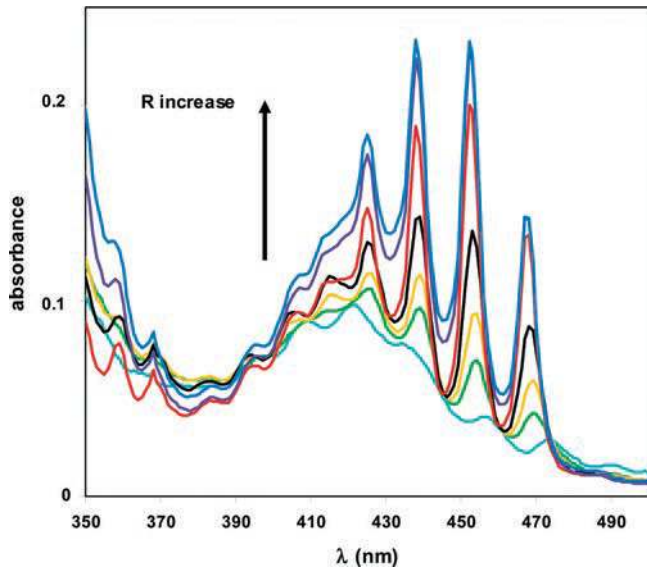


Figure 1. Absorption spectra for various values of R , the molar ratio $[\text{NO}_3^-]/[\text{UO}_2^{2+}]$, in $\text{C}_4\text{-mimTf}_2\text{N}$ (see text).

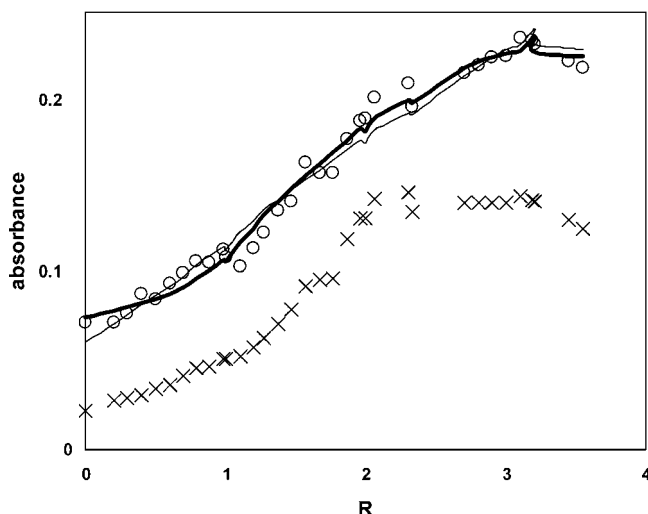


Figure 2. Variation of the absorbance as a function of R . O: $\lambda = 438$ nm; x: $\lambda = 467$ nm. Thick solid line: fit according to model I. Thin solid line: fit according to model II (see text).

and the matrix $\boldsymbol{\varepsilon}$ of the molar absorbance were fitting parameters for the minimization of the squares of the residuals

$$\Phi(\boldsymbol{\beta}, \boldsymbol{\varepsilon}) = \sum_{\lambda} \sum_{i=1}^n (A_{\text{exp}, \lambda, i} - A_{\lambda, i})^2 = \text{minimum} \quad (1)$$

where n is the number of experimental points and $A_{\text{exp}, \lambda}$ and A_{λ} are the experimental and calculated absorbances, respectively, for a given wavelength. The sets of data for the series of the wavelengths λ were merged together and treated simultaneously to calculate the $\boldsymbol{\beta}$ and $\boldsymbol{\varepsilon}$ values. In the program, the calculated absorbance A_{λ} is given by the Beer's equation

$$A_{\lambda} = A_{0\lambda} + l \sum_{j=1}^s \varepsilon_{\lambda j} C_j \quad (2)$$

Here, for a given wavelength λ , $A_{0\lambda}$ is the background absorption or systematic error, l is the optical path length (here, 1 cm), s

is the number of species involved in equilibrium, $\varepsilon_{\lambda j}$ is the molar absorbance of the j th species, and C_j is the equilibrium concentration of the j th species. The concentrations C_j as a function of the formation constants are expressed in Brinkley's form³³

$$C_j = \exp(\ln \beta_j + \sum_{k=1}^m \nu_{jk} \ln C_k) \quad (3)$$

where β_j is the overall stability constant of the j th product from m basic species (minimal set of reagents; here, two reagents UO_2^{2+} and NO_3^-) and ν_{jk} is the stoichiometric coefficient for a given reaction. Concentrations satisfy the mass-balance equations

$$\sum_{i=1}^s \nu_{ki} C_i = C_k^0 \quad k = 1, 2, \dots, m \quad (4)$$

where ν_{ki} is the stoichiometric coefficient of the k th basic species (UO_2^{2+} and NO_3^-) in the reaction in which the i th species is formed. As a criteria of reliability of the equilibrium model, we used the Hamilton's R factor³⁴ and residuals analysis ($A_{\text{exp}, \lambda} - A_{\lambda}$) versus A_{λ} .³⁵

CHEMEQUI uses three algorithms of minimization, rapid gradient method EQ with analytical presentation of derivatives $\partial \Phi / \partial \boldsymbol{\beta}$ and $\partial \Phi / \partial \boldsymbol{\varepsilon}$ ^{36,37} and reliable simplex³⁸ and Monte Carlo (low sensitivity to correlated calculated parameters)³⁹ approaches allowing one to significantly improve the reliability of the stability constant calculations. Details of the algorithms used in CHEMEQUI are given elsewhere.³² In the studied reagent concentration range, for estimations of highly correlated stability constants and related values, fitting algorithms of CHEMEQUI were extended by an option for cyclic fitting of the parameters one by one.

Experimental Results and Literature Review

Considering the pale-yellow color of $\text{C}_4\text{-mimNO}_3$, in a first step, the absorbance of $\text{C}_4\text{-mimNO}_3$ in $\text{C}_4\text{-mimTf}_2\text{N}$ was measured over the range of 200–800 nm for concentrations between 0 and 1 M (data not shown). The nitrate ions present an absorption band peaking at 309 nm, and the Beer's law appears to be perfectly verified at $\lambda = 309$ nm. By contrast, there is no significant absorption above 350 nm, up to 1 M. Therefore, in the calculations to follow, the specific absorption of the "free" nitrate ion (i.e., not complexed to uranyl) was not considered in the monowavelength approach, while a preliminary CHEMEQUI calculation demonstrated that the absorption of the nitrate ion is similar to the experimental error; therefore, it was not taken into account in further calculations.

Figure 1 displays selected spectra for R values varying between 0 and 3.5. As can be seen, the addition of nitrate ions to the $\text{UO}_2^{2+}/\text{C}_4\text{-mimTf}_2\text{N}$ solution leads to a tremendous increase of the signal above 420 nm, with the appearance of four well-defined bands at 425, 438, 453, and 467 nm. A small shoulder is present at 488 nm. These changes clearly evidence the complexation of UO_2^{2+} with NO_3^- . Figure 2 presents the absorbance variation as a function of R at $\lambda = 438$ nm, showing a leveling off above ~ 2.5 . As noted in the Experimental Section, according to the sample preparation, the uranyl concentration is not constant from one sample to another but is slightly decreasing while R is increasing, owing to the dilution effect.

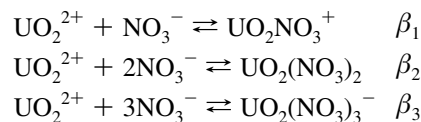
Such tremendous changes in the absorption spectra as a consequence of nitrate addition are well-documented in various solvents. They have been evidenced in water,^{21,23,40,41} water–acetone mixtures,²⁰ acetone,²⁵ acetonitrile,^{22,25} and various ionic liquids, either dry or not, C₄-mimTf₂N,^{23–26} C₄-mimPF₆, and Me₃NBuTf₂N²⁴ or C₄-mpyrTf₂N.²⁶ However, most of these works focused on the qualitative features of the absorption spectra, and besides the excellent paper of Ikeda and co-workers²² concerning complexation in acetonitrile, publications dealing with the determination of equilibrium constants and/or the stoichiometry of the successive uranyl–nitrate complexes and their individual spectra are scarce. In water, the reasons for such a lack of information are easily understandable. Owing to the strong affinity of water toward uranyl, even the first nitrate complexation is weak. Although various values can be found in the literature for all three complexation steps, with which a speciation diagram can be calculated,⁴⁰ the most reliable values to date are $K_1^\circ = 1.995 \text{ M}^{-1}$ and $K_2^\circ = 0.07 \text{ M}^{-1}$.⁴² This in turn explains why in most papers, only the first two complexes have been observed in water, by Raman⁴³ or fluorescence,⁴⁴ although a recent paper mentions the presence of the trinitrato uranyl complex in water as observed by UV–vis and EXAFS, but without any complexation constant values or speciation.⁴¹ It is possible that increasing temperature may favor complexation, but to our knowledge, in water, only the first nitrate complex has been investigated as a function of T .²¹ From the various UV–vis spectra displayed in the literature for the water case, it is clear that the two first complexes present the “characteristic” peaks already mentioned at 425, 438, 453, and 467 nm, the difference between the species being just a question of molar absorbance, not of shape or position. The same phenomenon has been observed in acetonitrile as the individual absorption spectra obtained by spectral decomposition²² show very similar peak positions for all three complexes, the molar absorbance of the 1:1 and 1:2 complexes being rather similar, while the 1:3 complex presents an absorption coefficient a factor of ~ 2 larger than the complexes of lower stoichiometry in the range of 420–480 nm. In ILs, information is even more limited. Besides the paper by Bradley et al.⁴⁵ displaying an almost featureless UV–vis spectra of U(VI) in pure liquid C₄-mimNO₃ (which corresponds to chemical conditions very different from ours), all available UV–vis data present the bands at 425, 438, 453, and 467 nm, but since these data have been obtained for a single U(VI)/NO₃[−] ratio of 4 (or values above $R = 4$ as in refs 26 and 23), no information can be deduced concerning the individual UV–vis absorption spectra of the (possible) successive complexes in ILs.

Other indications can be derived from EXAFS. Actually, EXAFS measurements performed for $R = 4$ ^{23,25} evidence that three nitrates on average are bound to uranyl. As EXAFS only gives access to averaged coordination numbers, it could be envisioned that this could be the weighted combination of various species, including the tetranitrato complex, but considering the steric hindrance of NO₃[−], this hypothesis can be ruled out. Similarly, EXAFS data point to two nitrates bound on average in the case of UO₂(NO₃)₂ dissolved in C₄-mimTf₂N.²⁴ However, contrary to the trinitrato complex, which is unambiguously evidenced through EXAFS, as already explained, this does not prove that UO₂(NO₃)₂ is the only species present in solution for $R = 2$, as discussed previously.^{24,41} In our recent work,⁴⁶ we have also obtained EXAFS data for $R = 1$, indicating one nitrate on average around uranyl, again with no definite proof of UO₂NO₃⁺ being alone in solution or in the presence of complexes of higher stoichiometry.

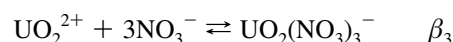
Modeling and Fitting Results

All together, data already found in the literature speak in favor of two different chemical interpretations, between which it is impossible to decide, (i) step-by-step complexation involving the species UO₂²⁺, UO₂NO₃⁺, UO₂(NO₃)₂, and UO₂(NO₃)₃[−] formed in accordance with three equilibria (model I) or (ii) starting from UO₂²⁺ ($R = 0$), less than three equilibria leading to the limiting complex UO₂(NO₃)₃[−] for $R \geq 3$ (model II). Chemically speaking, these two models can be written as follows

Model I:



Model II:



Other solutions are possible for model II, but we restrained our study to the sole case above as it differs widely from model I. Whatever the model chosen, it is deduced from EXAFS that for $R \geq 3$, the major component in the solution is the trinitrato complex, UO₂(NO₃)₃[−]. This has some implications on the value of β_3 .

It has to be noted that the way we write the various chemical equilibria envisioned to occur in C₄-mimTf₂N is most probably not an exact description of the real solvation sphere of the reacting species as we do not mention the solvent.¹⁰ MD calculations in dry ILs have repeatedly shown that the first coordination sphere of cations is mostly composed of the anions constituting the IL entity, with slight variations in the number of anions depending on the cation charge and the anion chemical structure.^{8,9,24} It should be recalled that the global charge of the entity composed of the cation and of its first solvation sphere in ILs is, most of the time, highly negative. It has also been shown that the second solvation sphere in ILs is also of importance, and the global charge of this entity is, by contrast, highly positive. In water, the notations UO₂²⁺, UO₂^{2+aq}, or UO₂^{2+·5H₂O} are equivalent, as far as mathematics is concerned, although the way to consider the solvation sphere is different from one to the other. By contrast, in ILs, the situation is unclear because the way the mass action law is expressed may change dramatically depending on how many solvation spheres are considered. The global charge of the reacting moieties varies depending on the choice made, which has implications for the mathematical expression of the activity coefficients. Finally, the way to express the activity of the IL solvent itself is not firmly assessed. As a consequence, and in order to conduct some fitting operations on the spectroscopic data that we collected, we decide to use “conditional” equilibrium constants, written as

$$\beta_i = [\text{UO}_2(\text{NO}_3)_i^{(2-i)}]/[\text{UO}_2^{2+}][\text{NO}_3^-]^i$$

where [X] represents the concentration of species X. In complex formation studies in aqueous solutions, it is very important to control the ionic strength of the solution, which is most of the time achieved by the addition of an inert salt in large quantities as compared to the reagents. In the case

TABLE 1: Calculated Stability Constants for the Complexation of UO_2^{2+} with NO_3^- and the Molar Absorbance Values of the Species in $\text{C}_4\text{-mimTf}_2\text{N}$ at 18.5°C^a

experimental data ^b : wavelengths, nm		$\log \beta_1$	$\log \beta_2$	$\log \beta_3$	HRF, % ^c
439, 440, 452, 453, 454, 466, 468		4.81 ± 0.45	8.31 ± 0.65	12.17 ± 0.81	2.56
molar absorbance ^d , $\text{cm}^{-1} \text{M}^{-1}$					
no.	wavelength, nm	ϵ_1	ϵ_2	ϵ_3	ϵ_4
1	439	3.25 (0.36)	9.47 (0.63)	12.7 (1.5)	13.73 (0.19)
2	440	4.18 (0.34)	8.06 (0.72)	24.2 (6.0)	18.18 (0.23)
3	452	4.13 (0.33)	5.35 (0.41)	7.2 (1.3)	12.31 (0.22)
4	453	3.92 (0.32)	5.80 (0.42)	1.8 (3.4)	10.60 (0.27)
5	454	5.78 (0.35)	12.08 (0.65)	12.2 (1.6)	18.80 (0.26)
6	466	7.46 (0.33)	9.45 (0.42)	12.1 (1.4)	18.58 (0.26)
7	468	7.25 (0.32)	9.78 (0.42)	6.0 (3.8)	16.26 (0.30)

^a Equilibria $\text{UO}_2^{2+} + \text{NO}_3^- = \text{UO}_2(\text{NO}_3)^+$, $\log \beta_1$; $\text{UO}_2^{2+} + 2\text{NO}_3^- = \text{UO}_2(\text{NO}_3)_2$, $\log \beta_2$; $\text{UO}_2^{2+} + 3\text{NO}_3^- = \text{UO}_2(\text{NO}_3)_3^-$, $\log \beta_3$.

^b Twenty-nine experimental data points for each wavelength. ^c Hamilton's R factor

$$\text{HRF} = 100 \left[\sum_{\lambda} \sum_{i=1}^n (A_{\text{exp},\lambda,i} - A_{\lambda,i})^2 / \sum_{\lambda} \sum_{i=1}^n (A_{\text{exp},\lambda,i})^2 \right]^{1/2}$$

See text for notation. ^d Molar absorbance: ϵ_1 [UO_2^{2+}], ϵ_2 [$\text{UO}_2(\text{NO}_3)^+$], ϵ_3 [$\text{UO}_2(\text{NO}_3)_2$], and ϵ_4 [$\text{UO}_2(\text{NO}_3)_3^-$]. Uncertainties are given as standard deviations in parentheses.

of ILs, supposing these media are mainly dissociated, the ionic strength should be in the range of 5–9 M (depending of the density of the used IL), owing to the cationic and anionic entities of which they are composed. Therefore, the complex formation occurring in our work should have a negligible impact on the total ionic strength as uranium is in the range of 10^{-2} M. Under this frame, the mathematical treatment of the models is feasible (see Data Fitting section).

In a first step, monowavelength fitting was achieved at $\lambda = 438$ nm. Model II was tested first as it contains fewer parameters than model I. As a rule, the data appeared to be fitted with similar χ^2 values for various sets of parameter values (β_3 , ϵ_0 , ϵ_3), where ϵ_i is the molar absorption coefficient of $\text{UO}_2(\text{NO}_3)_i^{(2-i)}$. This is due to the inherent correlation between these parameters in a monowavelength fitting. Owing to the average uncertainty in the coordination numbers as derived by EXAFS, the presence of $\text{UO}_2(\text{NO}_3)_3^-$ as a major species above $R = 3$ was taken into account by considering only fitting results for which the percentage of this species was calculated above 90% for $R \geq 3$. Given this condition, the fit leads to $\log \beta_3 = 10.8$ and $\epsilon_0 = 6.11$ and $\epsilon_3 = 23.9 \text{ cm}^{-1} \text{M}^{-1}$ (see Figure 2). In the case of model I, it has also been checked that mathematical solutions of the fit leading to $[\text{UO}_2(\text{NO}_3)_3^-] > 90\%$ for $R \geq 3$ are not the only ones to be obtained with very similar satisfying χ^2 values. Actually, as the data are rather smooth and the number of (correlated) parameters is important, this is not surprising. As an illustration, Figure 2 displays a fit of model II, for which $\text{UO}_2(\text{NO}_3)_3^-$ is equal to 87.5% of the total uranium concentration at $R = 3$ ($\log \beta_1 = 4.87$, $\log \beta_2 = 8.0$, and $\log \beta_3 = 11.8$; $\log K_1 = 4.87$, $\log K_2 = 3.13$, and $\log K_3 = 3.8$).

In a second step in a multiwavelength computation procedure, the CHEMEQUI program³² was used. Similarly, the main difficulty in the calculations of stability constants and molar absorbance values derived from the measured spectral data is the high correlation coefficients between the desired parameters, which lead to a shift of estimated parameters. To reduce the shifts of the parameters, a special module for their computations was developed and complemented in the CHEMEQUI program. In this procedure, only one parameter is fitted at each step. The procedure has systematically produced a cyclic optimization of fitting parameters one at a time. This procedure is repeated many

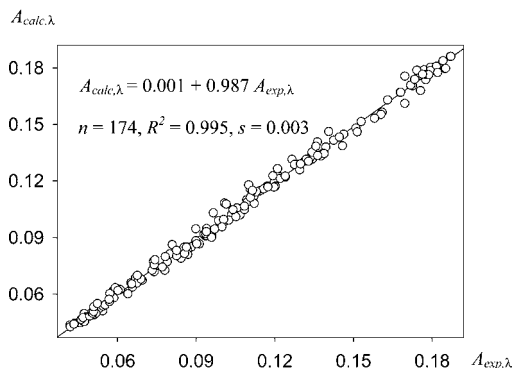


Figure 3. Calculated (solid line) versus experimental (symbols) values of absorbance for the model of formation of three complexes ML^+ , ML_2 , ML_3^- ($\text{M} = \text{UO}_2^{2+}$, $\text{L} = \text{NO}_3^-$) in the IL $\text{C}_4\text{-mimTf}_2\text{N}$. The CHEMEQUI calculations were performed on an experimental data set which includes seven data blocks for wavelengths 439, 440, 452, 453, 454, 466, and 468 nm.

times until a user-defined value of change of the Hamilton's R factor (HRF)

$$\text{HRF} = 100 \left[\sum_{\lambda} \sum_{i=1}^n (A_{\text{exp},\lambda,i} - A_{\lambda,i})^2 / \sum_{\lambda} \sum_{i=1}^n (A_{\text{exp},\lambda,i})^2 \right]^{1/2}$$

Taking into account the EXAFS results, the model of formation of three complexes ML^+ , ML_2 , and ML_3^- ($\text{M} = \text{UO}_2^{2+}$, $\text{L} = \text{NO}_3^-$) was analyzed. The stability constant calculations were performed on a reduced experimental data set, which included seven data blocks for wavelengths at 439, 440, 452, 453, 454, 466, and 468 nm. For each wavelength, 29 experimental data points were used. The selected bands in the absorption spectra correspond to the three sharp peaks which are most dependent on the reagent concentrations (Figure 1) and ensure minimal correlations between the estimated parameters. According to the Hamilton's R factor ($\text{HRF} = 2.56\%$; Table 1), we have found reasonable agreement between the calculated and experimental values of absorbances (Figure 3) for the model. The calculated stability constants ($\log \beta_1 = 4.81$, $\log \beta_2 = 8.31$ and $\log \beta_3 = 12.17$; $\log K_1 = 4.81$, $\log K_2 = 3.50$

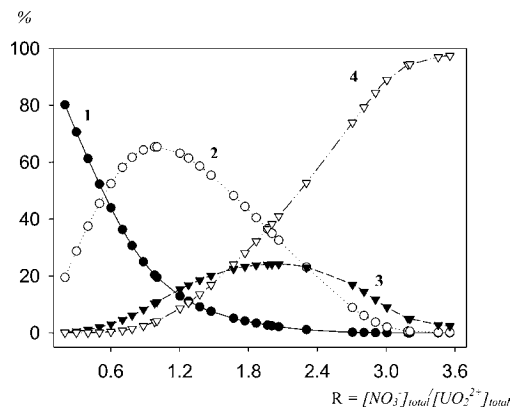


Figure 4. Percentage of the uranyl species as a function of the molar ratio R of the reagents for the complexation of UO_2^{2+} with NO_3^- in $\text{C}_4\text{-mimTf}_2\text{N}$. Data calculated by CHEMEQUI: UO_2^{2+} (1), $\text{UO}_2(\text{NO}_3)^+$ (2), $\text{UO}_2(\text{NO}_3)_2$ (3), and $\text{UO}_2(\text{NO}_3)_3^-$ (4); $[\text{UO}_2^{2+}]_{\text{total}} \approx 0.01 \text{ M}$.

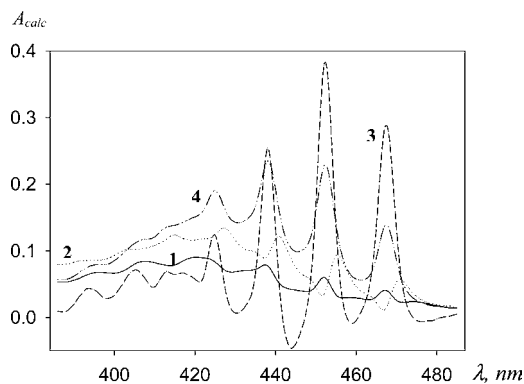


Figure 5. Calculated absorption spectra of the uranyl-containing species for a constant concentration of 0.01 M in $\text{C}_4\text{-mimTf}_2\text{N}$: UO_2^{2+} (1), $\text{UO}_2(\text{NO}_3)^+$ (2), $\text{UO}_2(\text{NO}_3)_2$ (3), and $\text{UO}_2(\text{NO}_3)_3^-$ (4).

and $\log K_3 = 3.86$) of formation of the species UO_2NO_3^+ , $\text{UO}_2(\text{NO}_3)_2$ and $\text{UO}_2(\text{NO}_3)_3^-$ in $\text{C}_4\text{-mimTf}_2\text{N}$ at $18.5 \text{ }^\circ\text{C}$ and the molar absorbances are presented in Table 1. The values of the stability constants as assessed by CHEMEQUI conform to the monowavelength fitting results, and the speciation (in percentage) of the uranyl species as a function of the molar ratio R of the reagents is in a good agreement with the EXAFS results (Figure 4). Thus, for a total concentration of $[\text{UO}_2^{2+}]_{\text{total}} = 0.01 \text{ M}$ and a molar ratio of $R = 1$, the reagents form mostly UO_2NO_3^+ , whereas at $R \geq 3$, the formation of the species $\text{UO}_2(\text{NO}_3)_3^-$ becomes dominant (Figure 4).

The values of the stability constants (Table 1) were utilized to calculate the molar absorbances of the uranyl-containing species and to derive their individual absorption spectra, using 3200 experimental data points including data blocks for 100 wavelengths from 384 to 485 nm. The calculated absorption spectra of the species $\text{UO}_2(\text{NO}_3)_2$ and $\text{UO}_2(\text{NO}_3)_3^-$ have the sharpest maxima at 438, 452, and 467 nm, whereas the medial size maxima of $\text{UO}_2(\text{NO}_3)^+$ are shifted to the long-wave side, up to 3–4 nm (Figure 5), which induces a shift and an enlargement of the peaks as this species is not negligible in the speciation.

Although these stability constants are conditional stability constants, as explained above, it would be possible to derive real thermodynamical stability constants provided the exact mathematical expression of mass action law in ILs is derived. Actually, the use of $\text{C}_4\text{-mimNO}_3$ and $\text{UO}_2(\text{Tf}_2\text{N})_2$ for the introduction of the reagents suppresses the presence of spectator ions, which is unavoidable in traditional molecular solvents. The

values of the stability constants derived in this work are much higher than the values obtained in water for the same system ($\log \beta_1 = 0.30$ and $\log \beta_2 = 0.31^{42}$), while they are closer to those derived in acetonitrile²² ($\log \beta_1 = 7.9$, $\log \beta_2 = 15.0$, and $\log \beta_3 = 20.0$), but no direct correlation can be found with the dielectric constants or polarization abilities of these solvents.⁴⁷ Nitrate ions appear to be strong complexing agents of uranyl in $\text{C}_4\text{-mimTf}_2\text{N}$, a situation which strongly resembles that of chloride ions toward transition-metal complexes, as evidenced by Dyson and co-workers.⁴⁸ Obviously, ILs induce very specific interactions favoring species with the highest possible stoichiometry. The successive complexation occurring in the system under study goes from a positively charged species, UO_2^{2+} , to a negatively charged species, $\text{UO}_2(\text{NO}_3)_3^-$, both embedded in an undefined number of solvation spheres of opposite sign at each rank. As we demonstrated for the first time that the determination of stability constants in ILs is feasible, we are now facing the challenging understanding of the (possibly mainly electrostatic) force fields that allow for such an efficient (i.e., with high stability constant values) complexation process in highly viscous liquids.

Conclusion

We have performed a comprehensive UV–vis study of the system $\text{UO}_2^{2+}/\text{NO}_3^-$ in the ionic liquid $\text{C}_4\text{-mimTf}_2\text{N}$. The conditional stability constants of the three successive complexes have been calculated and the individual absorption spectra derived for the first time in ILs. The use of dedicated salts ($\text{C}_4\text{-mimNO}_3$ and $\text{UO}_2(\text{Tf}_2\text{N})_2$) allowed us to work without spectator ions besides those composing the IL solvent itself, a situation unusual to molecular solvents. These results demonstrate that chemistry in ILs has reached a new step. The question of residual water content and impurities that were still problematic just a few years ago are now easily controlled, and it is possible to obtain reproducible and reliable data for rather intricate complexation chemistry pathways. With these data in hand and those for other systems to be studied, theoreticians will soon have the possibility to explore fundamental aspects of mass action law and activity coefficients in ILs.

Acknowledgment. This work has been performed under the financial support of “Groupement National de Recherche” PARIS, the European Network of Excellence (NoE) ACTINET, and the CNRS program “Chimie Pour un Développement Durable” (RdR3).

References and Notes

- (1) Wasserscheid, P.; Welton, T. *Ionic liquids in synthesis*; Wiley-VCH: Weinheim, Germany, 2008; Vol. 1 and 2.
- (2) Buzzeo, C. M.; Evans, G. R.; Compton, G. R. *ChemPhysChem* **2004**, *5*, 1106.
- (3) Dietz, L. M. *Sep. Sci. Technol.* **2006**, *41*, 2047.
- (4) Binnemans, K. *Chem. Rev.* **2007**, *107*, 2592.
- (5) Hao, J.; Zemb, T. *Curr. Opin. Colloid Interface Sci.* **2007**, *12*, 129.
- (6) Wilkes, S. J. *J. Mol. Catal. A: Chem.* **2004**, *214*, 11.
- (7) Cocalia, A. V.; Gutowski, E. K.; Rogers, D. R. *Coord. Chem. Rev.* **2006**, *250*, 755.
- (8) Chaumont, A.; Wipff, G. *Phys. Chem. Chem. Phys.* **2003**, *5*, 3481.
- (9) Schurhammer, R.; Wipff, G. *J. Phys. Chem. B* **2007**, *111*, 4659.
- (10) Billard, I.; Gaillard, C. *Radiochim. Acta* **2009**, *97*, 355.
- (11) Simonin, P. J.; Billard, I.; Hendrawan, H.; Bernard, O.; Lützenkirchen, K.; Sémon, L. *Phys. Chem. Chem. Phys.* **2003**, *5*, 520.
- (12) Abovsky, V.; Liu, Y.; Watanasiri, S. *Fluid Phase Equilib.* **1998**, *150–151*, 277.
- (13) Felmy, R. A.; Rai, D. *J. Solution Chem.* **1999**, *28*, 533.
- (14) Billard, I.; Mekki, S.; Gaillard, C.; Hesemann, P.; Moutiers, G.; Mariet, C.; Labet, A.; Bünzli, G. J. C. *Eur. J. Inorg. Chem.* **2004**, 1190.

- (15) Mekki, S.; Wai, M. C.; Billard, I.; Moutiers, G.; Burt, J.; Yen, H. C.; Wang, S. J.; Gaillard, C.; Ouadi, A.; Hesemann, P. *Chem.—Eur. J.* **2006**, *12*, 1760.
- (16) Gaillard, C.; Billard, I.; Chaumont, A.; Mekki, S.; Ouadi, A.; Denecke, M.; Moutiers, G.; Wipff, G. *Inorg. Chem.* **2005**, *44*, 8355.
- (17) Ouadi, A.; Klimchuk, O.; Gaillard, C.; Billard, I. *Green Chem.* **2007**, *9*, 1160.
- (18) Stumpf, S.; Billard, I.; Gaillard, C.; Panak, P.; Dardenne, K. *Radiochim. Acta* **2008**, *96*, 1.
- (19) Görrler-Walrand, C.; De Jaegere, S. *J. Chim. Phys.* **1972**, 726.
- (20) Azenha, E. M.; Burrows, D. H.; Formosinho, J. S.; Leitaó, P. M. L.; Miguel, G. M. *J. Chem. Soc., Dalton Trans.* **1988**, 2893.
- (21) Suleimenov, M. O.; Seward, M. T.; Hovey, K. J. *J. Solution Chem.* **2007**, *36*, 1093.
- (22) Ikeda, A.; Hennig, C.; Rossberg, A.; Tsushima, S.; Scheinost, C. A.; Bernhard, G. *Anal. Chem.* **2008**, *80*, 1102.
- (23) Billard, I.; Gaillard, C.; Hennig, C. *Dalton Trans.* **2007**, 4214.
- (24) Gaillard, C.; Chaumont, A.; Billard, I.; Hennig, C.; Ouadi, A.; Wipff, G. *Inorg. Chem.* **2007**, *46*, 4815.
- (25) Servaes, K.; Hennig, C.; Billard, I.; Gaillard, C.; Binnemans, K.; Van Deun, R.; Görrler-Walrand, C. *Eur. J. Inorg. Chem.* **2007**, 5120.
- (26) Nockemann, P.; Servaes, K.; Van Deun, R.; Van Hecke, K.; Van Meervelt, L.; Binnemans, K.; Görrler-Walrand, C. *Inorg. Chem.* **2007**, *46*, 11335.
- (27) Picquet, M.; Poinot, D.; Stutzmann, S.; Tkatchenko, I.; Tommasi, I.; Wasserscheid, P.; Zimmermann, J. *Topics Catal.* **2004**, *29*, 139.
- (28) Smiglak, M.; Holbrey, D. J.; Griffin, T. S.; Reichert, M. W.; Swatloski, P. R.; Katritsky, R. A.; Yang, H.; Zhang, D.; Kirichenko, K.; Rogers, D. R. *Green Chem.* **2007**, 9.
- (29) Billard, I.; Georg, S. *Helv. Chim. Acta* **2009**, *92*, 2227.
- (30) Adams, J. M. *Chemometrics in Analytical Spectroscopy*; The Royal Society of Chemistry: Cambridge, U.K., 1995.
- (31) Ouadi, A.; Gadenne, B.; Hesemann, P.; Moreau, E. J. J.; Billard, I.; Gaillard, C.; Mekki, S.; Moutiers, G. *Chem.—Eur. J.* **2006**, *12*, 3074.
- (32) Solov'ev, V.; Baulin, E. V.; Strakhova, N. N.; Kazachenko, P. V.; Belsky, K. V.; Varnek, A.; Volkova, A. T.; Wipff, G. *J. Chem. Soc., Perkin Trans.* **1998**, 1489.
- (33) Brinkley, R. S. *J. Chem. Phys.* **1947**, *15*, 107.
- (34) Hartley, R. F.; Burgess, C. *Solution equilibria*; Ellis Horwood Limited: Chichester, U.K., 1980.
- (35) Seber, A. G. *Linear hypothesis: a general theory*; Hafner: New York, 1966.
- (36) Novikov, P. V.; Ignateva, I. T.; Raevskii, A. O. *Zh. Neorg. Khim.* **1986**, *31*, 1474.
- (37) Novikov, P. V.; Raevskii, A. O. *Izv. Akad. Nauk.* **1983**, 1336.
- (38) Himmelblau, D. M. *Applied non linear programming*; McGraw-Hill Book Company: Austin, TX, 1972.
- (39) Conley, W. *Int. J. Math. Educ. Technol.* **1981**, *12*, 609.
- (40) Houwer, D. S.; Görrler-Walrand, C. *J. Alloys Compd.* **2001**, *323/324*, 683.
- (41) Ikeda-Ohno, A.; Hennig, C.; Tsushima, S.; Scheinost, C. A.; Bernhard, G.; Yaita, T. *Inorg. Chem.* **2009**, *48*, 7201.
- (42) Ruas, A.; Bernard, O.; Caniffi, B.; Simonin, P. J.; Turq, P.; Blum, L.; Moisy, P. *J. Phys. Chem. B* **2006**, *110*, 3435.
- (43) Nguyen-Trung, C.; Begum, M. G.; Palmer, A. D. *Inorg. Chem.* **1992**, *31*, 5280.
- (44) Couston, L.; Pouyat, D.; Moulin, C.; Decambox, P. *Appl. Spectrosc.* **1995**, *49*, 349.
- (45) Bradley, E. A.; Hardacre, C.; Nieuwenhuyzen, M.; Pitner, R. W.; Sanders, D.; Seddon, R. K.; Thied, C. R. *Inorg. Chem.* **2004**, *43*, 2503.
- (46) Gaillard, C.; Chaumont, A.; Billard, I.; Hennig, C.; Ouadi, A.; Georg, S.; Wipff, G. 2009, submitted.
- (47) Reichardt, C. *Green Chem.* **2005**, *7*, 339.
- (48) Daguinet, C.; Dyson, J. P. *Organometallics* **2004**, *23*, 6080.

JP9107624